*33rd EPS Conference on Plasma Phys. Rome, 19 - 23 June 2006 ECA Vol.**30I**, P-5.022 (2006)*

Kinetic simulations of electron gas in the presence of SRS

M. Mašek[1], K. Rohlena[1]

[1] *Institute of Physics, A.S.C.R., Prague, Czech Republic*

In a few last decades experimental and theoretical studies of nanosecond intense laser beam propagation through the plasma corona became very intense in order to understand what processes influence the formation of plasma corona. This knowledge is very important for numerous experimental situations including the thermonuclear fusion experiments, particularly with the indirect drive, where the laser beam after entering the hohlraum faces a developed well underdense plasma inside [1], and the production of high charge ion, in which an electrostatic waves growing due to parametric instabilities accelerate particles which, in turn, speed up the plasma corona expansion and thus contribute to the enhanced charge freezing effect [2]. This paper is devoted to a numerical study of stimulated Raman scattering of impinging laser beam. During the propagation of laser pulse through a well underdense plasma in a self-generated corona, a high-amplitude longitudinal electron plasma wave and a transverse electromagnetic wave are resonantly generated. In a 1D geometry two scattering processes are possible: forward (SRS-F) and backward (SRS-B), where in both the processes the electron plasma wave (in the case of SRS-B with the trapping ability) is propagating in the direction of the laser beam. The particle trapping effects the wave propagation in a dual way: (1) by a modification of the collisionless damping. The wobbling motion involves alternating acceleration and deceleration of the trapped electrons in the frame moving with the wave and it is thus invalidating the Landau damping mechanism, which is intrinsically connected with the acceleration of electrons by the potential crests of the wave. With the damping absent the energy coming from the primary wave is leading to a growth of the scattered wave and consequently it causes a secondary scattering can occur - cascading [3]. (2) by a modification of the dispersion curve. The trapped electrons are closely tied to the potential troughs of the carrier electrostatic wave causing thus in their interval of the phase space a substantial deviation from the overall Maxwell velocity distribution. This, in turn, means a different dynamic description of their motion reflected in a perturbation of electrostatic potential of the carrier wave modulated by the wobble frequency. This may lead to the trapped particle instability (TPI) and a growth of sidebands [4, 5], which is translated in the appearance of a new branch of dispersion curve of the electrostatic plasma wave, [3]. Due to the TPI the sidebands with a lower wave number grow preferentially mainly because of a higher Landau damping rate of the wave modes with higher wave numbers. As a consequence the electrostatic peak is broadening during the simulation and it is moving to the left of the spectrum. These wave modes have a somewhat higher phase velocity than the resonant wave mode, but lie well within the bulk of pre-accelerated electrons. These modes influence then quite a large amount of electrons in the phase space, which results in a significant broadening of plateau on the electron distribution function. Other situation occurs in the case of SRS-F, whose electrostatic daughter wave has usually the phase velocity comparable with the speed of light, thus it cannot influence the electrons in the non-relativistic plasmas directly but only via its non-linear combination with the SRS-B plasma wave. Thus is leading to a formation of the electrostatic quasi-modes [6] with the “phase velocity” lying within the bulk of the electron distribution.

The presented results are based on the spatially 1D periodical kinetic model solving the Vlasov equation together with the full set of Maxwell equations. The fundamental 1D equation set for a weakly collisional homogeneous laser plasma can be written as follows

$$\frac{\partial f}{\partial t}+v_x\frac{\partial f}{\partial x}+\frac{e}{m}\left(\frac{\partial \varphi}{\partial x}-\frac{e}{m}A\frac{\partial A}{\partial x}\right)\frac{\partial f}{\partial v_x}=\nu_c\left(\frac{\partial (v_x f)}{\partial v_x}+<v_x^2>\frac{\partial^2 f}{\partial v_x^2}\right), \qquad (1)$$

$$\left[\frac{\partial^2}{\partial x^2} - \frac{1}{c^2}\frac{\partial^2}{\partial t^2} - \frac{\omega_{pe}^2}{c^2}\frac{n_e}{n_0}\right]A = 0, \tag{2}$$

$$\frac{\partial^2 \varphi}{\partial x^2} = \frac{e}{m}(n_e - n_0), \tag{3}$$

$$\frac{n_e}{n_0} = \int_{-\infty}^{\infty} f \, dv. \tag{4}$$

In the Vlasov equation the velocity in the perpendicular direction is replaced by the mean oscillatory velocity in the field of incident laser light $v_y = eA/m$. The simplified Fokker-Planck collision term on the right-hand side of the Vlasov equation was included, where ν_c is the effective collision frequency. Numerically such a term also provides a satisfactory stabilization of the method, which is helpful in carrying the solution to sufficiently long times. (1)-(4) is a closed set of equations, which was solved numerically by the transform method [7].

The physical parameters of the model including the effective collision frequency are inspired by conditions relevant to the PALS facility. The initial electron temperature is thus chosen $T_e = 10^7\ K \simeq 0.9\ keV$, and the density is 4.4 % of the critical density at the considered laser wavelength in vacuum $\lambda_{vac} = 1.315\ \mu m$. The electron plasma frequency and the Debye length corresponding to these values are $\omega_{pe} = 3.0 \times 10^{14}\ s^{-1}$ and $\lambda_D = 4.1 \times 10^{-8}\ m$. The incident power density of the laser beam is estimated to be $I = 10^{20}\ W/m^2$. For the numerical stabilization of the method the collision frequency $\nu_c/\omega_{pe} = 0.05$ is sufficient, which is a realistic value for high-Z plasmas. The initial distribution is assumed to be Maxwellian and the initial electron density perturbations are set as a low-level white noise.

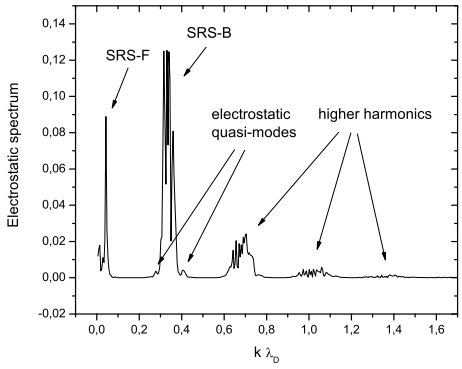

Figure 1: A fully developed electrostatic k-spectrum in the nonlinear stage of SRS with the spectral broadened peak of SRS-B due to the present TPI. A shift of the central EPW belonging to SRS-B towards the lower side-band is clearly seen.

By solving the matching conditions for the SRS together with the linear dispersion relations for the participating waves for SRS-B, one obtains ($\omega_0/\omega_{pe} = 4.774$, $k_0\lambda_D = 0.192$), ($\omega_s/\omega_{pe} = 3.618$, $k_s\lambda_D = 0.143$), ($\omega_e/\omega_{pe} = 1.156$, $k_e\lambda_D = 0.334$). In the case of SRS-F the values of the frequencies and wave numbers of the scattered electromagnetic wave and of the plasma wave are ($\omega_s/\omega_{pe} = 3.771$, $k_s\lambda_D = 0.149$), ($\omega_e/\omega_{pe} = 1.003$, $k_e\lambda_D = 0.042$). Very similar results were obtained from the full Vlasov-Maxwell numerical model, as it can be easily seen in Fig. 1, where the electrostatic k-spectrum is depicted at $\omega_{pe}t = 300$. At this time the nonlinear stage of SRS is reached and the electrostatic spectrum is fully developed. The most significant peak in the spectrum corresponds to the SRS-B plasma wave. This plasma wave has the phase velocity well within the bulk of electrons on the velocity distribution ($v_{ph}/v_T = 3.45$), so it is strongly interacting with a large amount of particles in the vicinity of its phase velocity. As the amplitude of the plasma wave grows, the trapping region in the phase space is developing and the particles inside this region are becoming trapped in the potential minima of the wave. This is visualized as a strong perturbation in the phase space near the phase velocity, which is, however, changing in space and time, and the plateau on the distribution is recovered only after a space averaging. The non-linear stage of the Landau damping (caused by the interaction of the trapped particles with the plasma wave) leads to a saturation of the wave growth (see Fig. 2).

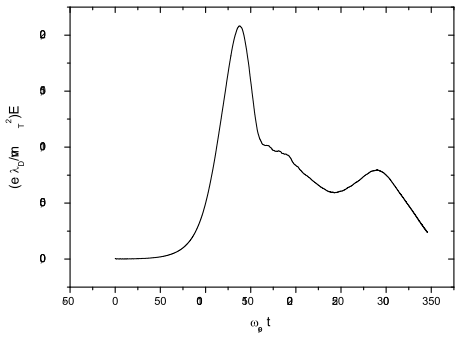

Figure 2: The temporal evolution of the SRS-B electron plasma wave.

Since in the discrete k-spectrum of the numerical model the matching conditions are not fulfilled exactly, a growth of several modes with their wave numbers near the resonance is recorded. The energy of the laser pump is thus distributed between these few modes. A high amplitude of the mode, which is the closest to the resonance, leads to a strong "wave-wave" interaction with nearby modes and to their significant growth. Fig. 2 shows that at $\omega_{pe}t = 170$ the SRS-B plasma wave amplitude decrease is stopped, but soon after a following decrease of the amplitude occurs. We interpret it in connection with the trapped particle instability. In the resonant SRS-B electrostatic wave the wobbling electron cause a strong modification of the electron density which leads to a generation of unstable sidebands of the main electrostatic daughter wave, while the amplitude of the central mode is decreasing as its energy is transfered to the sidebands (see Fig. 2). Due to the Landau damping, a stronger growth is recorded in the case of sidebands on the left from the central mode and also the center of the wave packet moves to the left.

Since the electron motion in the potential trough of the wave can be described by the monokinetic fluid approximation characterized by the bouncing frequency $\omega_B = \sqrt{eEk/m_e}$ we can estimate the half-width of the spectral line in the k-spectrum to be $\delta k \approx \omega_B / v_{ph}$. This estimate calculation gives for the spectral broadening in our case $\delta k \lambda_D = 0.049$. In fact, a more accurate description of the TPI gives a strong dependence of the spectral broadening on the fraction of trapped particle [4]. Following the procedure of the paper [4] we can numerically calculate the TPI dispersion relation for the conditions of the PALS experiment with the parameters obtained from the numerical simulation. From the simulation fraction of trapped particles at $\omega_{pe}t = 170$ can be taken as $f_T = 0.122$. Under these conditions the computed dispersion curve is shown in Fig. 3 (a). As it is obvious in the Fig. 3 (a) that the modes with the wave numbers $k\lambda_D = 0.235$ and $k\lambda_D = 0.435$ have the maximum growth. Their growth rates predicted by the linear theory are approximately $\gamma/\omega_{pe} = 0.045$. For a comparison we present temporal behaviour of one of these modes obtained from the full Vlasov-Maxwell simulation showed in Fig. 3 (b). From this curve, the growth rate of sideband is estimated to be $\gamma/\omega_{pe} = 0.027$. A certain disagreement of the values obtained from the linear theory and from the full model is caused by collisions added to the full model for the numerical stabilization, which are not accounted for in the linear theory.

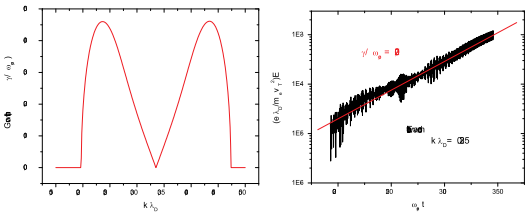

Figure 3: (a) Imaginary part of TPI dispersion curve expresses a dependence of the TPI growth rate on the wave number. (b) Temporal evolution of the sideband ($k\lambda_D = 0.235$) obtained from the Vlasov-Maxwell simulation.

More interesting is the significant shift in the phase velocity of the sidebands. The phase velocity increases considerably with the decreasing wave number and the sideband with the highest growth rate on this side of dispersion curve has the phase velocity approximately $v_{ph}/v_T = 4.5$. It becomes clear that with the growing amplitudes of the sidebands the wave spectrum expands and the plateau on the electron distribution function broadens. This stage of the system evolution a large amount of electrons is influenced by these wave modes which results in their

trapping and acceleration. This process is demonstrated in Fig. 4. A formation of huge plateau in the averaged electron velocity distribution with the fraction of trapped particles $f_T = 25.9$ % can be seen.

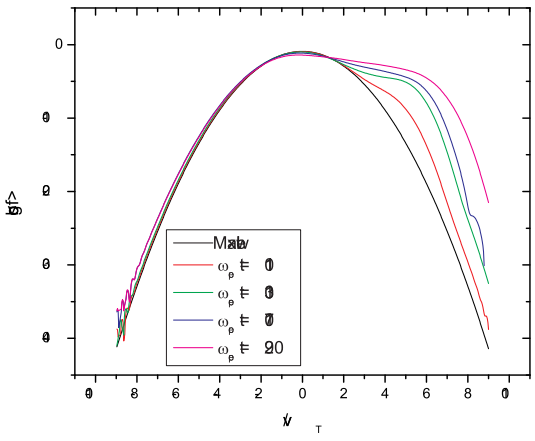

Figure 4: The formation of huge plateau on EDF is demonstrated at $\omega_{pe}t = 110$, 130, 170, and 290 by spatially averaging.

The narrow peak close to the beginning of the horizontal coordinate corresponds to the electrostatic daughter wave of SRS-F. This plasma wave has a very high phase velocity, which is comparable to the speed of light (in our case $v_{ph}/v_T = 23.6$). It can interact with the particles only indirectly by combining with the SRS-B electron plasma wave. There are two possible quasi-modes. These modes have the wave numbers $k\lambda_D = 0.273$ and $k\lambda_D = 0.403$ (see Fig. 1). A high frequency difference between SRS-B and SRS-F plasma wave causes very different phase velocities of the both quasi-modes ($v_{ph}/v_T = 0.5$ and $v_{ph}/v_T = 5.7$, respectively). While the phase velocity of the first of them lies in the region of the phase space, where most of the electrons are present, the second one has its phase velocity far away from the bulk of electrons in the statistical equilibrium. However, at the moment when this electrostatic quasi-mode has a significant amplitude ($\omega_{pe}t \approx 250$), the electrons are yet accelerated by the processes described above and they can interact with it. Thanks to this interaction the plateau on the electron distribution expands as presented in Fig. 4.

The following mechanisms were illustrated by the results of the numerical modeling and some of them are interpreted by model calculations on the level of linear theories.
(1) The electrostatic daughter wave of the back-scattered Raman wave leads to strong electron trapping in its potential minima, which leads to a saturation of the wave growth. (2) The electrostatic daughter wave of the forward-scattered Raman wave cannot interact with the plasma electrons directly owing to its high phase velocity, but it can combine with its partner generated by the Raman back-scattering to form a non-resonant quasi-mode capable of electron trapping. (3) The wobbling of the trapped electrons in the potential minima of the electrostatic back-scattering daughter wave leads to a modulation of the electron density and to a generation of unstable sidebands of the main electrostatic daughter wave. (4) In later times the lower sideband takes over from the main wave, which is gradually outgrown, and the sideband even forms its own quasi-mode with the daughter wave of the forward scatter.

Support by the grant No. 202/05/2745 of the Grant Agency of the Czech Republic is gratefully acknowledged.

References

[1] J. Lindl, Phys. Plasmas **2**, 3933 (1995)
[2] K. Rohlena *et al.*, Laser Part. Beams **14**, 335 (1996)
[3] A. Salcedo *et al.*, Nucl. Fusion **43**, 1759 (2003)
[4] W. L. Kruer *et al.*, Phys. Rev. Lett. **15**, 838 (1969)
[5] S. Brunner *et al.*, Phys. Rev. Lett. **93**, 145003 (2004)
[6] L. Krlín, Czech. J. Phys. **B 31**, 383 (1981)
[7] T, P. Armstrong *et al.*, in *Methods in Computational Physics vol. 9*, (London: Academic Press) p. 29-86 (1970)